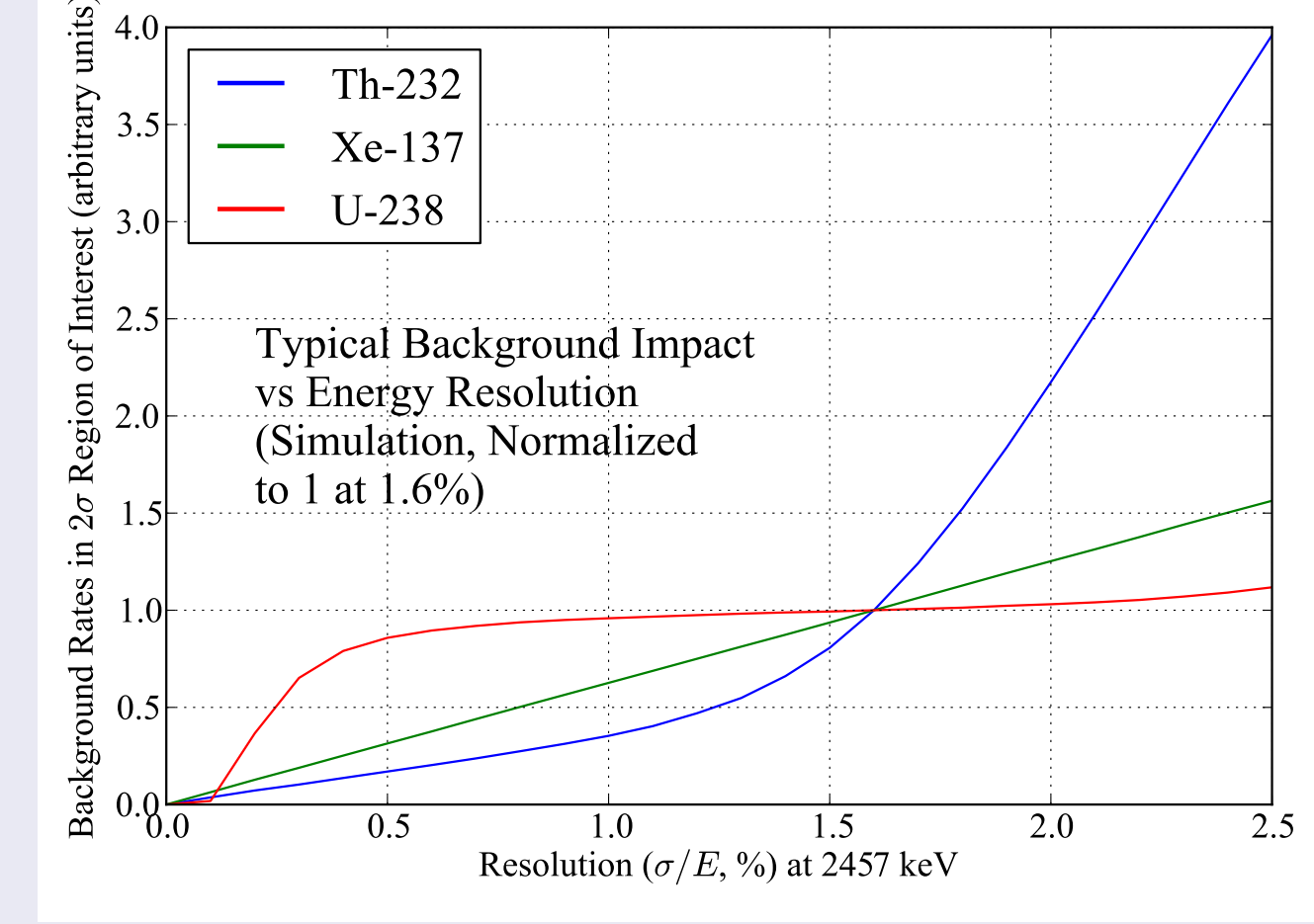
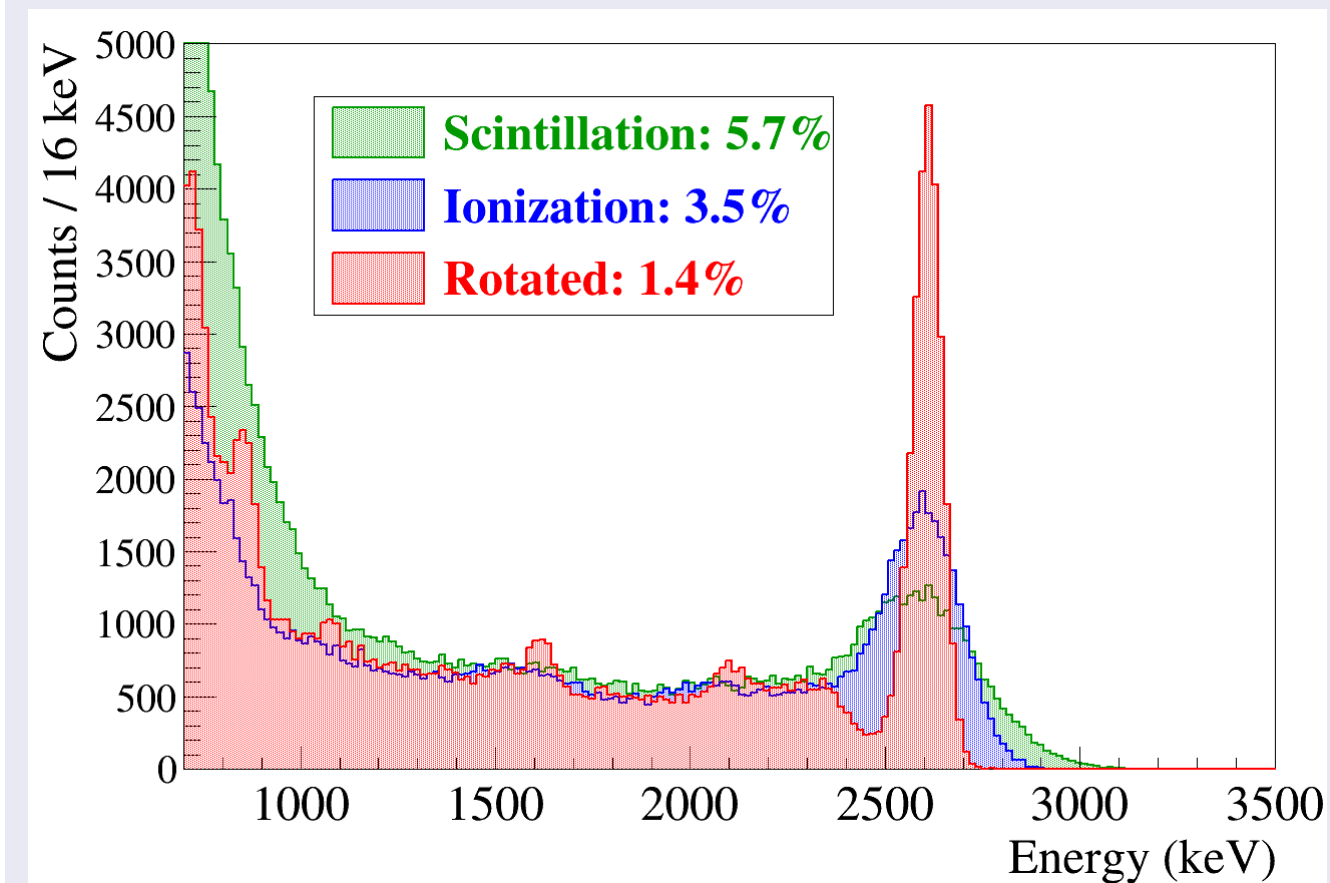
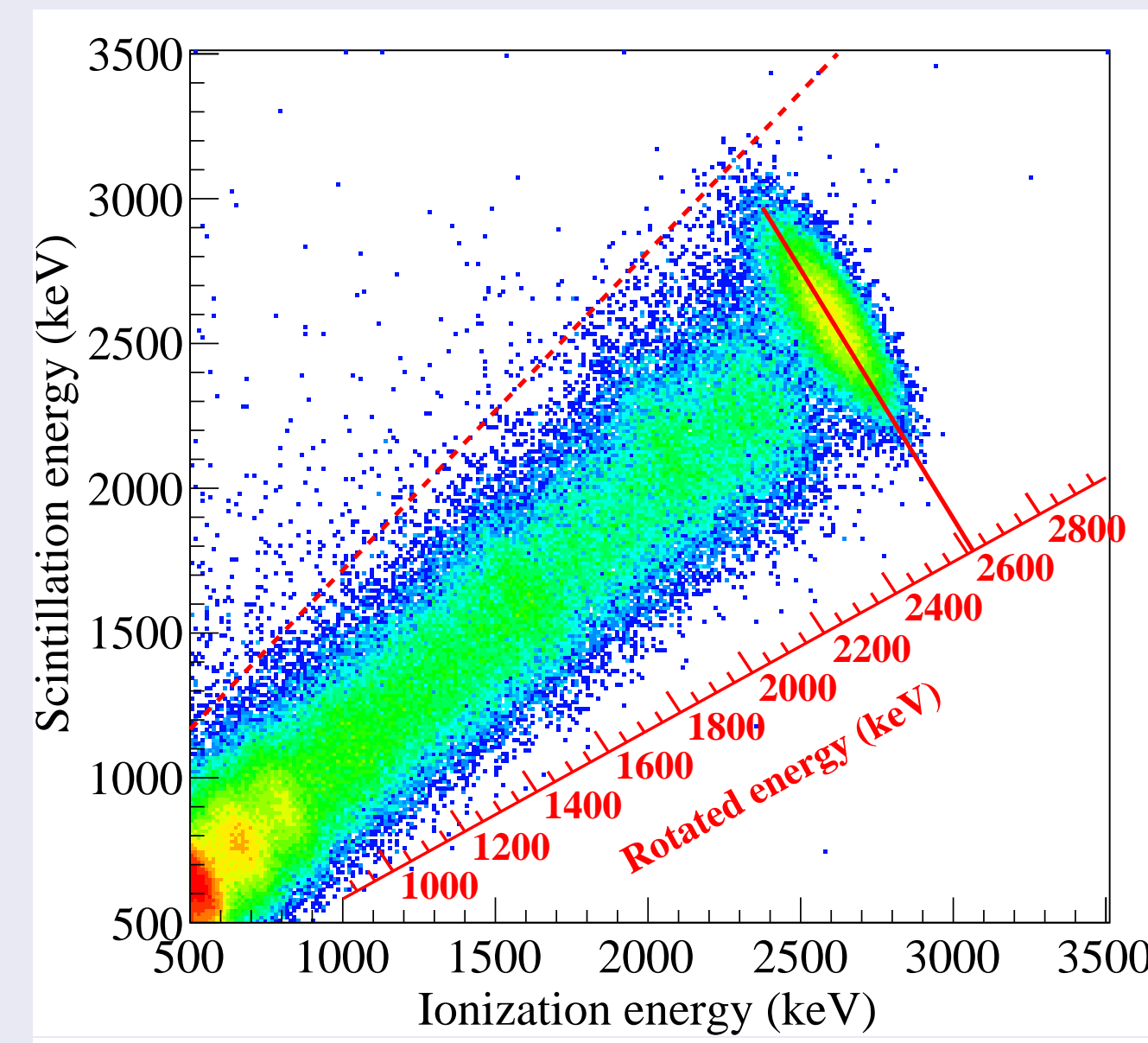
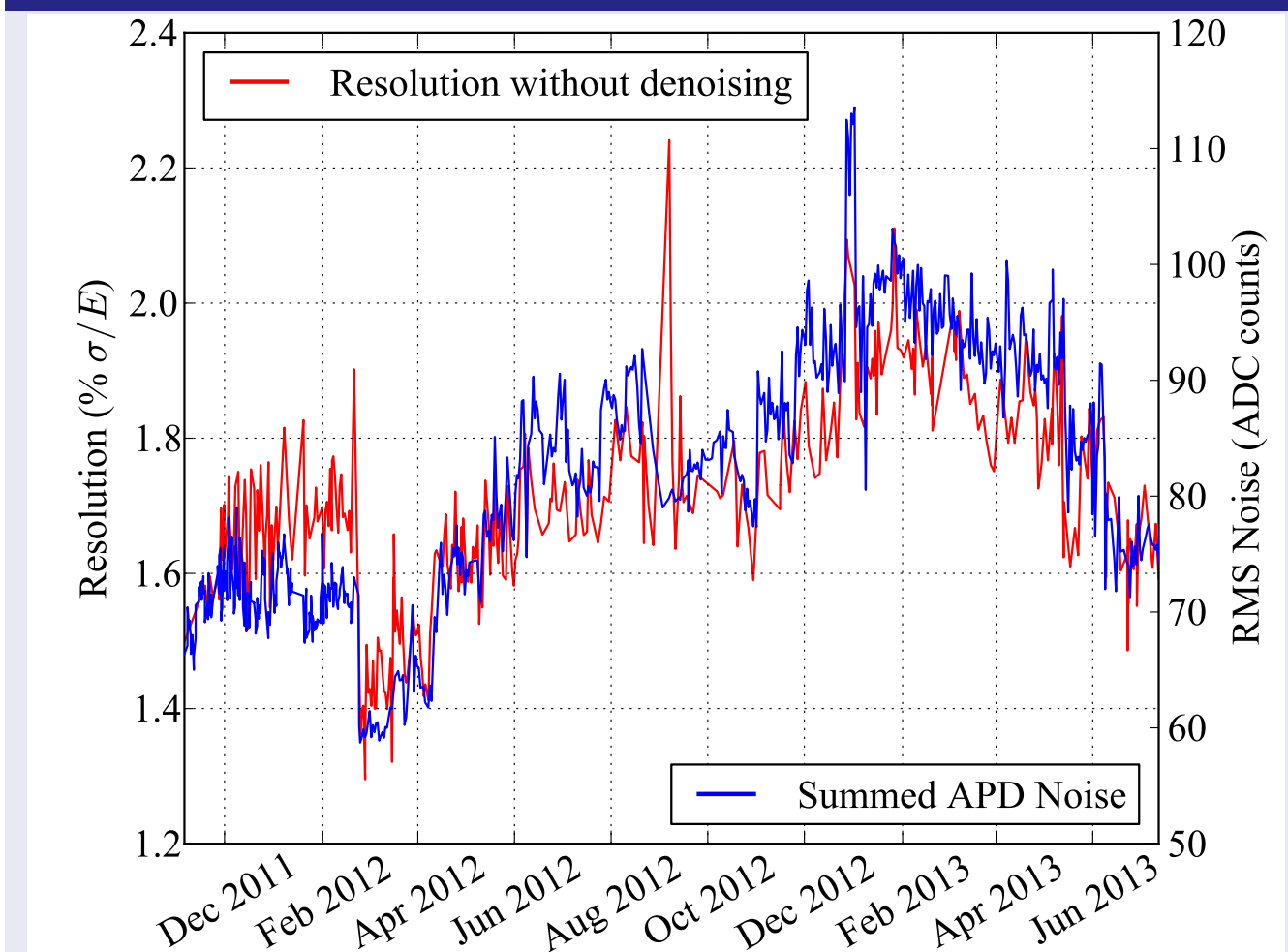


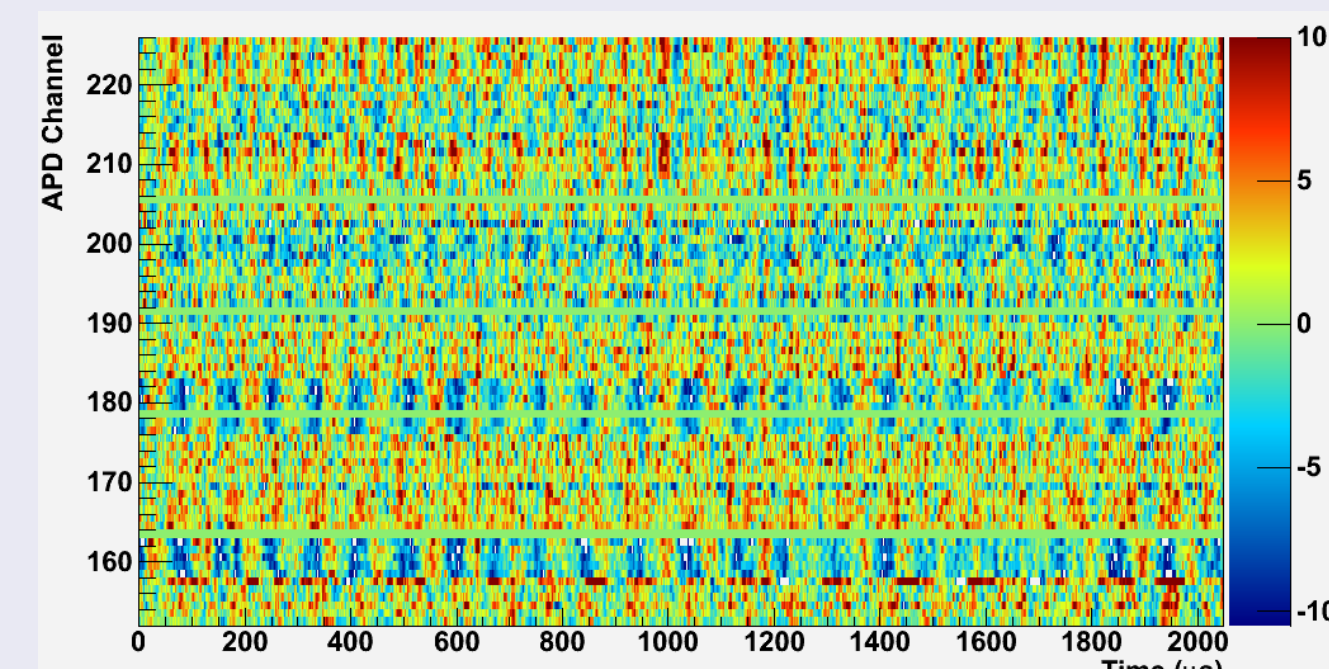
The EXO-200 TPC has 110 kg of liquid xenon, enriched to 80.6% in ^{136}Xe . The xenon is continuously purified. The TPC consists of a cathode in the middle and two anodes on the ends.



APD Noise Limits Resolution



Noise on the APD waveforms is highly correlated across channels. Individual channels are dominated by Poisson statistics on the signal; only when they are summed together does electronic noise become dominant. We want a denoising scheme which simultaneously minimizes signal fluctuations and electronic noise.



APD Denoising in EXO-200

by Clayton G. Davis
on behalf of the EXO-200 Collaboration

Model of a Waveform

When there is one energy deposit in the xenon, the APD waveform $X_i[f]$ (in frequency space) on channel i can be modeled:

$$X_i[f] = M_i Y_i[f] + N_i[f], \text{ where:}$$

- $Y_i[f]$ is the unit-magnitude template pulse for channel i .
- M_i is the pulse magnitude; it measures the scintillation energy, corrupted by Poisson fluctuations in photon statistics and gain.
- $N_i[f]$ is the additive (electronic) noise on channel i .

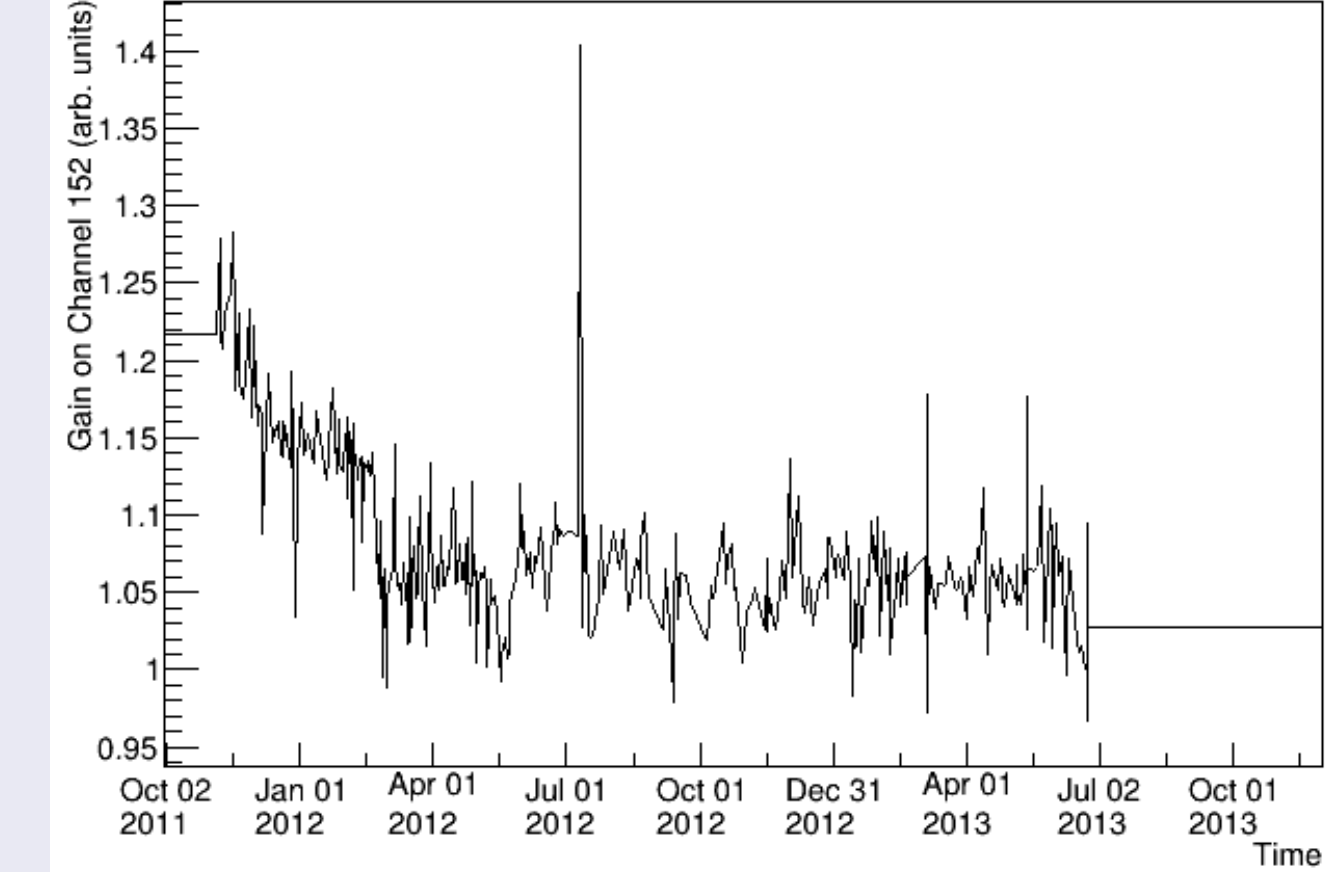
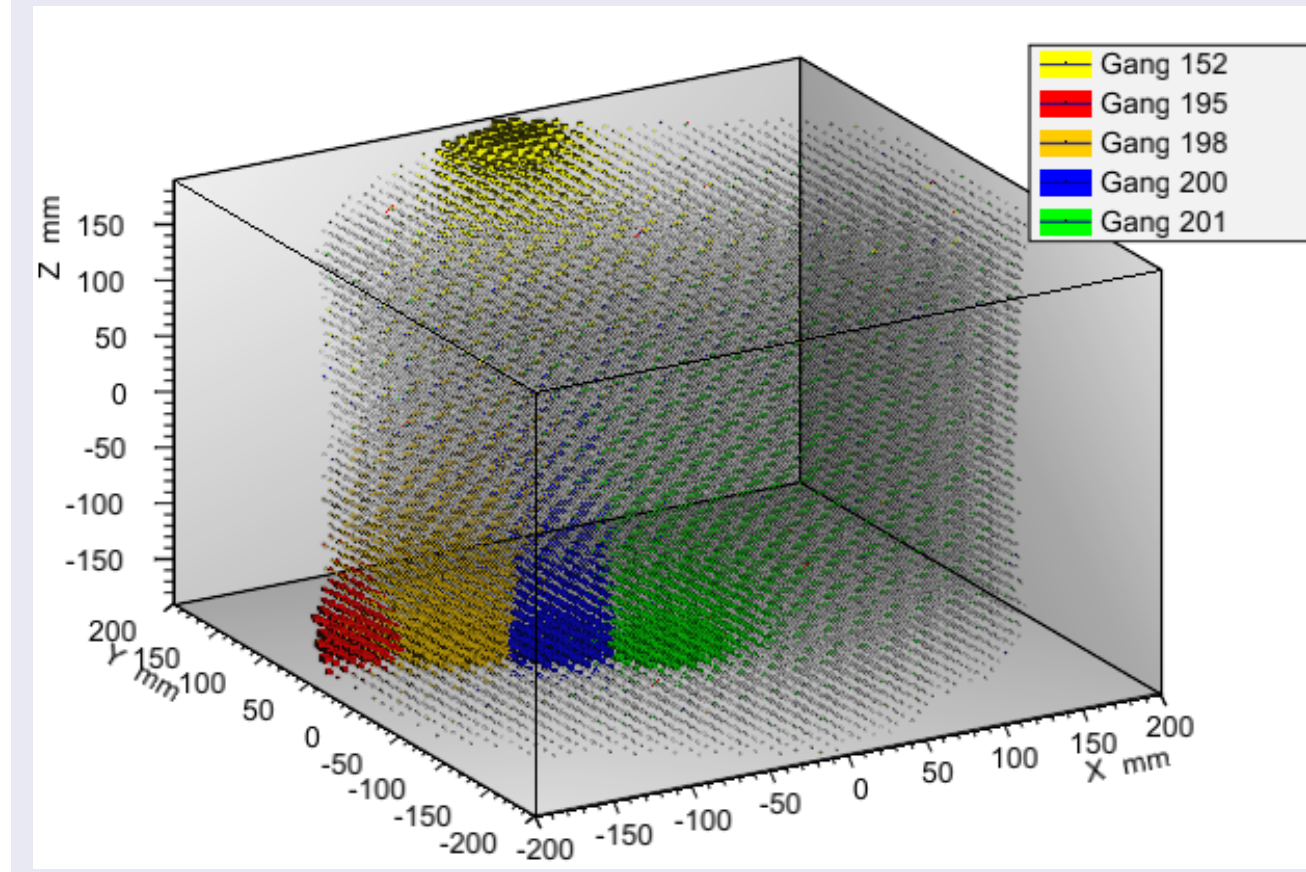
Characterizing the Lightmap

We need a map of light yield versus deposit position for each channel to model the dependence of M_i on energy. Channels have time-dependent gain, so each channel i needs a lightmap function $L_i(\vec{x}, t)$. Very difficult to measure this empirically with limited source statistics.

However, we can make a simplifying assumption that L_i is separable into a position-dependent and time-dependent component representing photon propagation through the detector and gain variations over time. This lets us simplify:

$$L_i(\vec{x}, t) = R_i(\vec{x}) S_i(t)$$

and we only need to empirically measure $R_i(\vec{x})$ and $S_i(t)$ for each channel – much easier.



Characterizing the Noise

In general, we could characterize the noise to lowest order by measuring the correlations:

$$\langle N_i[f] N_j[g] \rangle \text{ for each channel } i, j \text{ and frequency } f, g.$$

However, our noise is dominated by electronics and is relatively steady over short time periods; pairwise correlations will be zero when $f \neq g$. So, we only need to characterize correlations:

$$\langle N_i[f] N_j[f] \rangle \text{ for each channel } i, j \text{ and frequency } f.$$

Note that if we had significant dark current, we might be dominated by terms like $\langle N_i[f] N_i[g] \rangle$ instead.

The beauty of a low-background detector is that it collects lots of noise, so measuring noise empirically is relatively easy.

Optimal Energy Estimator

The goal is to find the optimal linear estimator of energy E . The estimator must be real-valued, so we describe it with parameters $A_i[f]$ and $B_i[f]$ and estimate the energy as:

$$\hat{E} = \sum_{if} A_i[f] \tilde{X}_i^R[f] + B_i[f] \tilde{X}_i^I[f].$$

We constrain the estimator to be unbiased:

$$\langle E - \hat{E} \rangle = 0.$$

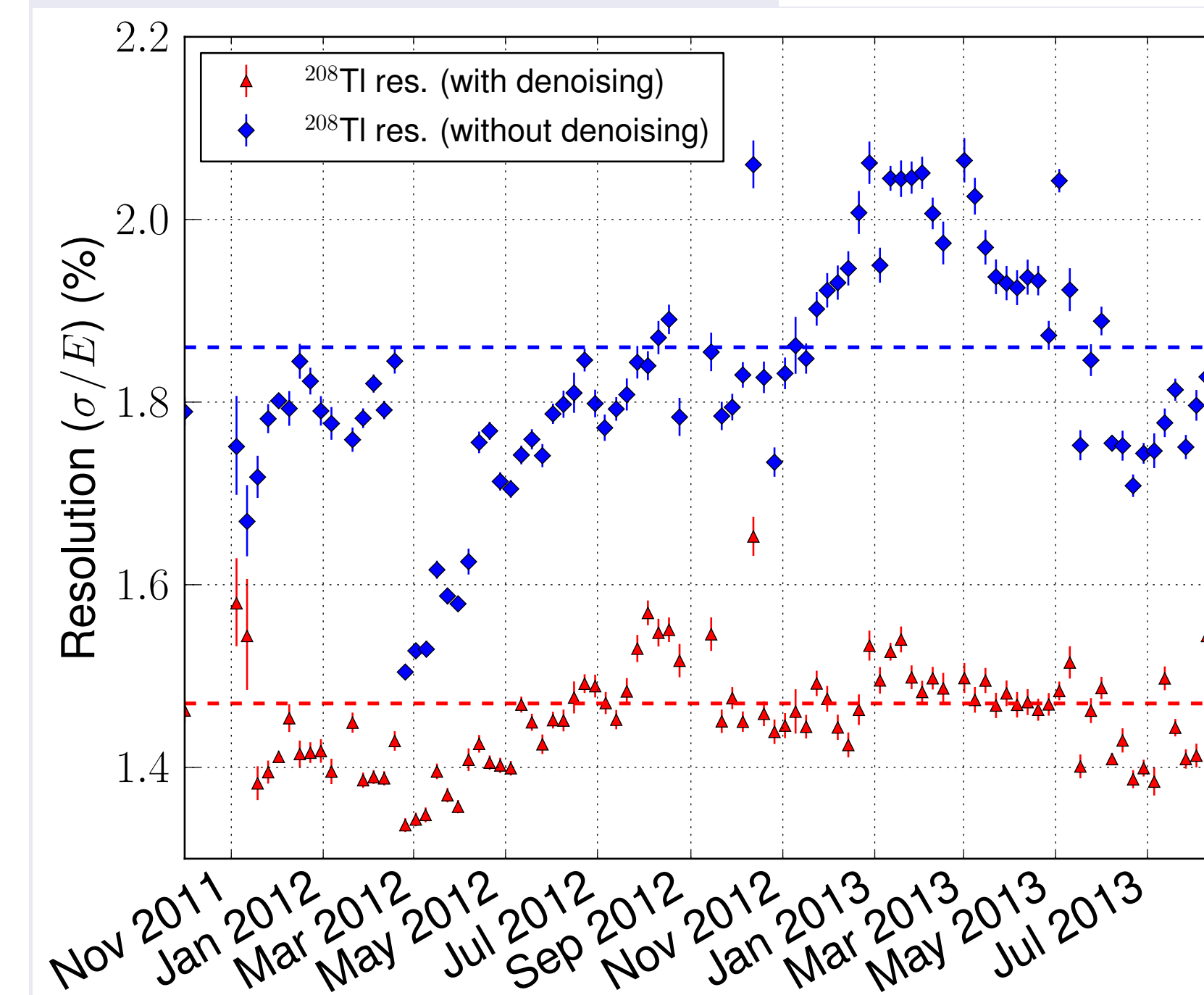
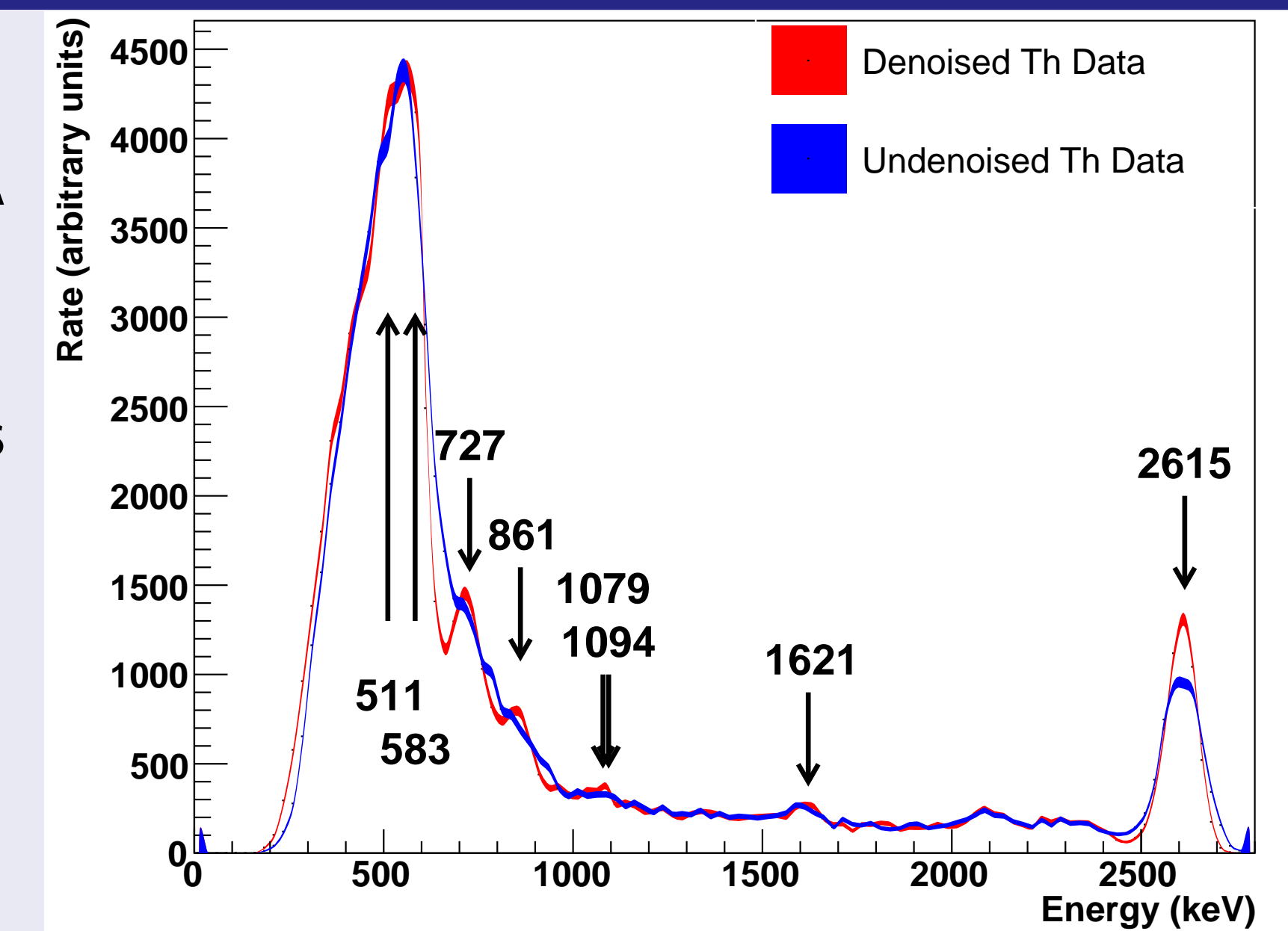
The optimal choice of $A_i[f]$ and $B_i[f]$ is the one which minimizes the mean square error,

$$\langle (E - \hat{E})^2 \rangle.$$

We can do this: it requires us to solve a large matrix equation, and since every event is different each one requires its own solution, but for a low-statistics detector this is feasible. And it has been done.

Impact on Spectra

The resolution is visibly improved at all energies. A ^{228}Th source spectrum (right) shows the primary peak at 2615 keV becomes narrower and taller, and some low-energy peaks become visible which before blended into the smooth background.



The strong time-dependence in resolution which we see before denoising has flattened out after denoising. This is consistent with the expectation that time-dependence comes from noise, and that denoising removes much of that noise.

Descriptions here.

